An Equation of State Compositional Model

Keith H. Coats, SPE, Intercomp Resource Development and Engineering Inc.

Abstract

This paper describes an implicit, three-dimensional formulation for simulating compositional-type reservoir problems. The model treats three-phase flow in Cartesian (x-y-z) or cylindrical (r-θ-z) geometries. Applicability ranges from depletion or cycling of volatile oil and gas condensate to miscible flooding operations involving either outright or multicontact-miscibility.

The formulation uses an equation of state for phase equilibrium and property calculations. The equation of state provides consistency and smoothness as gas- and oil-phase compositions and properties converge near a critical point. This avoids computational problems near a critical point associated with use of different correlations for K values as opposed to phase densities.

Computational testing with example multicontact-miscibility (MCM) problems indicates stable convergence of this formulation as phase properties converge at a critical point. Results for these MCM problems show significant numerical dispersion, primarily affecting the calculated velocity of the miscible-front advance. Our continuing effort is directed toward reduction of this numerical disperson and comparison of model results with laboratory experiments for both MCM and outright-miscibility cases.

We feel that the implicit nature of the model enhances efficiency as well as reliability for most compositional-type problems. However, while we report detailed problem results and associated computing times, we lack similar reported times to compare the overall efficiency of an implicit compositional formulation with that of a semi-implicit formulation.

0197-7520/80/0010-8284$00.25

Introduction

Many papers have treated increasingly sophisticated or efficient methods for numerical modeling of black-oil reservoir performance. That type of reservoir allows an assumption that reservoir gas and oil have different but fixed compositions, with the solubility of gas in oil being dependent on pressure alone.

A smaller number of papers have presented numerical models for simulating isothermal "compositional" reservoirs, where oil and gas equilibrium compositions vary considerably with spatial position and time. With some simplification, the reservoir problems requiring compositional treatment can be divided into two types. The first type is depletion and/or cycling of volatile oil and gas condensate reservoirs. The second type is miscible flooding with MCM generated in situ.

A distinction between these types is that the first usually involves phase compositions removed from the critical point, while the second type generally requires calculation of phase compositions and properties converging at the critical point. A compositional model should be capable of treating the additional problem of outright miscibility where the original oil and injected fluid are miscible on first contact.

A difficulty in modeling the MCM process is achievement of consistent, stable convergence of gas- and oil-phase compositions, densities, and viscosities as the critical point is approached. A number of studies[1-5] have reported models that use different correlations for equilibrium K-values as opposed to phase densities. Use of an equation of state offers the advantage of a single, consistent source of calculated K-values, phase densities, and their densities near a critical point.

The purpose of this work was to develop, and test with sample problems, a multidimensional, com-

positional model using an equation of state. While this objective includes applicability to depletion, cycling, and outright miscible-flooding operations, our emphasis in this work was placed on simulation of the MCM process

Van Quy *et al.*[6] described a one-dimensional, two-phase (gas/oil), compositional model neglecting gravity and capillary forces. They used a three-component correlation guaranteeing consistency of phase compositions and properties at the critical point and presented detailed calculated, and some experimental, one-dimensional results for vaporizing and condensing (MCM) gas injection cases. Corteville *et al.*[7] used the same model and presented additional comparisons between linear calculated and experimental results.

Metcalfe *et al.*[8] and Fussell *et al.*[9] published studies using a cell-to-cell flash calculation model[10] to simulate the MCM or vaporizing gas injection process. Fussell and Yanosik[11] described iterative methods for phase equilibria calculations using a modified Redlich-Kwong equation of state. Fussell and Fussell[12] used Ref. 11 in developing a formulation for a multidimensional compositional model. They presented an example calculation for an immiscible gas injection case.

This paper describes an equation-of-state implicit compositional model formulation for three-dimensional, three-phase flow under viscous, gravity, and capillary forces. Test applications to one- and two-dimensional MCM-type problems are described. This paper reports the capability of this formulation in computationally coping with the convergence problems encountered near critical points in the MCM process. Our continuing effort is directed toward comparisons with published experimental data, for both MCM and outright-miscibility processes, and further examination and reduction of numerical dispersion error.

General Description of the Model

The model formulation treats one, two-, or three-dimensional flow of water, oil, and gas in x, y, and z formations of heterogeneous permeability and porosity with Cartesian (x-y-z) or cylindrical (r-θ-z) geometries. The fluid flow is simulated using Darcy's law, incorporating gravity, viscous, and capillary forces. Relative permeability and capillary pressure are dependent on saturations and interfacial tension.

The model applies to depletion of volatile oil or gas condensate reservoirs and cycling of the latter. However, the primary objective of this work was development and testing of a model capable of simulating vaporizing gas-injection and miscible-flooding operations. In the following test applications, we emphasize the MCM process.

The model consists of mass balances for water and N_c hydrocarbon components and associated constraint equations. Oil- and gas-phase densities and fugacities or K-values are calculated from a modified Redlich-Kwong equation of state.[13,14] Oil- and gas-phase viscosities are calculated from the Lohrenz *et al.* method[15] and converge to a common value as the phase compositions converge near a critical point. Interfacial tension is calculated from the Macleod-Sugden correlation.[16]

The formulation is implicit and requires simultaneous solution of a set of $N_c + 1$ finite difference equations throughout the grid representing the reservoir. This implicit formulation requires more arithmetic (computing time) per grid block per time step than an IMPES (implicit pressure, explicit saturation) type of model. However, the latter treats transmissibilities explicitly in saturation and composition variables and accordingly tends to require smaller and more time steps than an implicit model. We have not yet compared overall efficiencies of the two types of models.

Formulation assumptions are instantaneous equilibrium between gas and oil phases in any grid block and mutual insolubility of water and hydrocarbon components. There are no assumptions or limits on the number of hydrocarbon components, other than computer storage and computing time requirements. Diffusion is neglected.

Material balance error for each component is printed after calculation as

(initial-in-place + cumulative injection
− cumulative production − actual-in-place)
÷ max (cumulative injection
− cumulative production),

where all quantities are in moles. This fractional error is consistently less than ± 0.0001.

PVT treatment of fluid and rock properties is described in the Appendix.

Mathematical Model Description

The model consists of N equations written in finite difference form for each grid block, where N is $2N_c + 4$. The N_c component mass balances are

$$\frac{V}{\Delta t}\,\delta\left[\phi(\rho_o S_o x_i + \rho_g S_g y_i)\right] = \Delta\left[\Upsilon \rho_o x_i \frac{k_{ro}}{\mu_o}\left(\Delta p - \Delta P_{cgo} - \gamma_o \Delta Z\right)\right] + \Delta\left[\Upsilon \rho_g y_i \frac{k_{rg}}{\mu_g}\left(\Delta p - \gamma_g \Delta Z\right)\right] - q_i\,,$$
$$i = 1, 2, \ldots, N_c\,. \quad \ldots\ldots\ldots\ldots\ldots\ldots (1)$$

The water mass balance is

$$\frac{V}{\Delta t}\,\delta(\phi \rho_w S_w) = \Delta\left[\Upsilon \rho_w \frac{k_{rw}}{\mu_w}\left(\Delta p - \Delta P_{cgo} - \Delta P_{cwo} - \gamma_w \Delta Z\right)\right] - q_w\,. \quad \ldots\ldots\ldots (2)$$

The N_c fugacity constraints,

$$f_i^L - f_i^V = 0, \quad i = 1, 2, \ldots, N_c\,, \quad \ldots\ldots\ldots (3)$$

express the requirement that liquid- and vapor-phase fugacities must be equal for each component. The two mole fraction constraints

$$\sum_{i=1}^{N_c} x_i = 1.0 \,, \quad \ldots\ldots\ldots\ldots\ldots\ldots \text{(4a)}$$

and

$$\sum_{i=1}^{N_c} y_i = 1.0 \,, \quad \ldots\ldots\ldots\ldots\ldots\ldots \text{(4b)}$$

and the saturation constraint

$$S_o + S_g + S_w = 1.0 \,, \quad \ldots\ldots\ldots\ldots\ldots\ldots \text{(5)}$$

complete the set of N model equations.

The N unknowns corresponding to these equations are

$$x_1, x_2, \ldots, x_{N_c}; \; y_1, y_2, \ldots, y_{N_c};$$

$$p, S_o, S_g, S_w \quad \ldots\ldots\ldots\ldots\ldots\ldots \text{(6)}$$

These unknowns are referred to hereafter as $\{P_i\}$, where $P_1 = x_1$, $P_2 = x_2$, ..., $P_N = S_w$, in the order listed in Eq. 6.

To solve these N equations, all terms must be expanded into linear combinations of the selected dependent variables or unknowns. In the implicit formulation described here, the N unknowns at each time step are $\{\delta P_i\}$ for each grid block.

For any quantity or product of terms X, our notation is

$$\delta X \equiv X_{n+1} - X_n \quad \ldots\ldots\ldots\ldots\ldots\ldots \text{(7a)}$$

and

$$\delta X = X^{\ell+1} - x^{\ell} \,, \quad \ldots\ldots\ldots\ldots\ldots\ldots \text{(7b)}$$

where subscript n denotes time level, X_n is known because all variables are known at the old time level, and superscript ℓ is iterate number. Thus, δX is the change in X over the time step, while δX is the change in X over one iteration.

The time difference is approximated by

$$\delta X \cong \delta X + X^{\ell} - X_n \,, \quad \ldots\ldots\ldots\ldots\ldots\ldots \text{(8)}$$

which becomes an exact equality as $X^{\ell+1} \to X_{n+1}$. Implicit treatment of interblock flow and well terms and quantities in the constraints simply consists of expressing the terms at time level $n+1$:

$$X_{n+1} \cong X^{\ell+1} = X^{\ell} + \delta X \,. \quad \ldots\ldots\ldots\ldots\ldots\ldots \text{(9)}$$

Finally, the term δX is expanded as a linear combination of the N dependent variables or unknowns $\{P_i\}$ as

$$\delta X \cong \sum_{j=1}^{N} \left(\frac{\partial X}{\partial P_j}\right)^{\ell} \delta P_j \,, \quad \ldots\ldots\ldots\ldots\ldots\ldots \text{(10)}$$

where the derivatives are evaluated at the latest iterate values of $\{P_i\}$. Derivatives of products of terms are obtained by the normal chain rule,

$$\frac{\partial (abc)}{\partial P} = \left(bc \frac{\partial a}{\partial P} + ac \frac{\partial b}{\partial P} + ab \frac{\partial c}{\partial P}\right). \quad \ldots\ldots\ldots\ldots \text{(11)}$$

Expansion of Accumulation Terms

The time-difference or accumulation terms on the left side of the mass balances are expanded as illustrated here for component i.

$$\delta\left[\phi(\rho_o S_o x_i + \rho_g S_g y_i)\right] = \left[\phi(\rho_o S_o x_i + \rho_g S_g y_i)\right]^{\ell} - \left[\phi(\rho_o S_o x_i + \rho_g S_g y_i)\right]_n + \sum_{j=1}^{N} \frac{\partial}{\partial P_j}\left[\phi(\rho_o S_o x_i + \rho_g S_g y_i)\right]^{\ell} \delta P_j \,, \quad \ldots\ldots\ldots\ldots\ldots\ldots \text{(12)}$$

where, for illustration,

$$\frac{\partial}{\partial x_j}\left[\phi(\rho_o S_o x_i + \rho_g S_g y_i)\right] = \phi S_o\left(\rho_o \delta_{ij} + x_i \frac{\partial \rho_o}{\partial x_j}\right), \quad \ldots\ldots\ldots\ldots \text{(13)}$$

$$\frac{\partial}{\partial p}\left[\phi(\rho_o S_o x_i + \rho_g S_g y_i)\right] = \phi\left(S_o x_i \frac{\partial \rho_o}{\partial p} + S_g y_i \frac{\partial \rho_g}{\partial p}\right) + \left(\rho_o S_o x_i + \rho_g S_g y_i\right) \frac{\partial \phi}{\partial p} \,, \quad \ldots\ldots\ldots\ldots\ldots\ldots \text{(14)}$$

and δ_{ij} is the Dirac delta function.

Expansion of Interblock Flow Terms

The interblock flow terms on the right sides of the mass balances are evaluated implicitly, as illustrated for x direction flow of Component i in the gas phase between adjacent Grid Blocks 1 and 2:

$$\Upsilon_x \rho_g y_i \frac{k_{rg}}{\mu_g}\left(\Delta p - \gamma_g \Delta Z\right) = \Upsilon_x\left[\rho_g y_i \frac{k_{rg}}{\mu_g}\left(\Delta p - \gamma_g \Delta Z\right)\right]^{\ell} + \Upsilon_x \sum_{j=1}^{N} \frac{\partial}{\partial P_j}\left[\rho_g y_i \frac{k_{rg}}{\mu_g}\left(\Delta p - \gamma_g \Delta Z\right)\right]^{\ell} \delta P_j \,. \quad \ldots\ldots\ldots\ldots\ldots\ldots \text{(15)}$$

k_{rg}, μ_g, ρ_g, and y_i are evaluated at the upstream block and

$$\gamma_g = \omega \gamma_{g1} + (1-\omega)\gamma_{g2} \,, \quad \ldots\ldots\ldots\ldots\ldots\ldots \text{(16)}$$

where

$$\omega = V_1 \phi_1 / (V_1 \phi_1 + V_2 \phi_2) \quad \ldots\ldots\ldots\ldots \text{(17)}$$

if S_g is nonzero in both grid blocks. If S_g is nonzero only in the upstream block, then γ_g is evaluated upstream.

Treatment of Well Terms

We illustrate the semi-implicit treatment of well terms for production of Component i from a well on deliverability completed in Layers $k = 1$, 2, and 3. The rate of production from Layer k is

$$q_{i,k} = \mathrm{PI}_k \left\{ \left[\left(\rho_o \frac{k_{ro}}{\mu_o} x_i + \rho_g \frac{k_{rg}}{\mu_g} y_i\right)_k \cdot \left(p_k - p_{wbk}\right)\right]^{\ell} + \sum_{j=1}^{N} \frac{\partial}{\partial P_j}\left[\left(\rho_o \frac{k_{ro}}{\mu_o} x_i + \rho_g \frac{k_{rg}}{\mu_g} y_i\right)_k \left(p_k - p_{wbk}\right)\right]^{\ell} \delta P_j \right\}. \quad \ldots \text{(18)}$$

The wellbore pressure gradient is calculated using an explicit wellbore gradient as

$$p_{wbk} = p_{wb,k-1} + \bar{\gamma}(Z_k - Z_{k-1}) , \quad \ldots\ldots\ldots (19)$$

where p_{wbl} = the specified bottomhole flowing pressure, Z_k is subsea depth opposite the center of Layer k, and

$$\bar{\gamma} = \Big[\sum_{k=1}^{3} \mathrm{PI}_k (\lambda_o \gamma_o + \lambda_g \gamma_g + \lambda_w \gamma_w) p_k \Big/ \sum_{k=1}^{3} \mathrm{PI}_k (\lambda_o + \lambda_g + \lambda_w) p_k \Big]_n . \quad \ldots\ldots (20)$$

Expansion of Constraint Equations

The fugacity constraints (Eq. 3) are approximated implicitly (at Time Level $n+1$) using

$$f_{i,n+1} \cong f_i^{\ell} + \sum_{j=1}^{2N_c+1} \left(\frac{\partial f_i}{\partial P_j} \right)^{\ell} \delta P_j , \quad \ldots\ldots\ldots (21)$$

where f_i is dependent only on mole fractions and pressure and is independent of saturations. Use of Eq. 21 in Eq. 3 gives

$$\sum_{j=1}^{2N_c+1} \frac{\partial}{\partial P_j} \left(f_i^L - f_i^V \right)^{\ell} \delta P_j = \left(f_i^V - f_i^L \right)^{\ell} ,$$

$$i = 1, 2, \ldots, N_c . \quad \ldots\ldots\ldots\ldots (22)$$

Of course, f_i^L is dependent only on $\{x_i\}$ and p and f_i^V are dependent only on $\{y_i\}$ and p. The constraints are expressed implicitly as

$$\sum_{i=1}^{N_c} \delta x_i = 1.0 - \sum_{i=1}^{N_c} x_i^{\ell} , \quad \ldots\ldots\ldots\ldots (23a)$$

$$\sum_{i=1}^{N_c} \delta y_i = 1.0 - \sum_{i=1}^{N_c} y_i^{\ell} , \quad \ldots\ldots\ldots\ldots (23b)$$

$$\delta S_o + \delta S_g + \delta S_w = 1.0 - (S_o + S_g + S_w)^{\ell} . \quad \ldots (24)$$

Consolidation of N Model Equations

When written for a given grid block, the first $N_c + 1$ of the N model equations (Eqs. 1 through 5) involve unknowns $\{\delta P_j\}$ for that grid block and in addition involve the unknowns $\{\delta P_j\}$ of each neighboring block. This appearance of adjacent-block unknowns is a result of the interblock flow terms present in the mass balances. We refer to these $N_c + 1$ mass balances as the "primary" equations. The remaining $N_c + 3$ (constraint) equations (Eqs. 3 through 5) involve only the unknowns $\{\delta P_j\}$ of the given grid block. Therefore, they can be used to eliminate $N_c + 3$ unknowns from the primary equations, resulting in a set of $N_c + 1$ primary equations in $N_c + 1$ unknowns.

The expanded constraint equations (Eqs. 22, 23a, and 23b) are $N_c + 2$ equations in $2N_c + 1$ unknowns: $\{x_i\}$, $\{y_i\}$, and pressure, p. We use Gaussian elimination to solve for the $N_c + 2$ unknowns ($\{\delta x_i\}$, δy_1, and δy_2) in terms of the remaining $N_c - 1$ unknowns (δy_3, δy_4, ..., δy_{N_c}, δp). Thus,

$$\begin{Bmatrix} \delta x_1 \\ \delta x_2 \\ \vdots \\ \delta x_{N_c} \\ \delta y_1 \\ \delta y_2 \end{Bmatrix} = \begin{bmatrix} a_{1,1} & a_{1,2} \ldots a_{1,N_c-1} \\ a_{2,1} & a_{2,2} \ldots a_{2,N_c-1} \\ \vdots & \\ a_{N_c+2,1} & \ldots\ldots a_{N_c+2,N_c-1} \end{bmatrix} \times \begin{Bmatrix} \delta y_3 \\ \delta y_4 \\ \vdots \\ \delta y_{N_c} \\ \delta p \end{Bmatrix} + \begin{Bmatrix} b_1 \\ b_2 \\ \vdots \\ b_{N_c+2} \end{Bmatrix} . \quad \ldots (25)$$

The mass-balance equations (Eqs. 1 and 2) with terms expanded as described above, are $N_c + 1$ equations in the $2N_c + 4$ unknowns $\{\delta P_j\}$. Eq. 25 is used to eliminate the $N_c + 2$ unknowns $\{\delta x_1, \delta x_2, \ldots, \delta x_{N_c}, \delta y_1, \delta y_2\}$ and Eq. 24 is used to eliminate δS_w. This elimination of $N_c + 3$ unknowns leaves a set of $N_c + 1$ primary (mass balance) equations in $N_c + 1$ unknowns. This set of equations can be written in matrix form as

$$C\,\underline{\delta P} = \Delta(\Upsilon \Delta \underline{\delta P}) + \underline{R} , \quad \ldots\ldots\ldots\ldots (26)$$

where C and Υ are $(N_c + 1) \times (N_c + 1)$ matrices, $\underline{\delta P}$ is the column vector $\{\delta y_3, \delta y_4, \ldots, \delta y_{N_c}, \delta S_g\}$, and $\underline{R}$ is an $(N_c + 1) \times 1$ column vector consisting of residual terms dependent on the latest iterate values of fluid and rock properties. These primary equations are solved by the reduced-bandwidth direct-solution technique described by Price and Coats.[17]

After solution of Eq. 26 for $\underline{\delta P}$, the eliminated unknowns $\{\delta x_1, \delta x_2, \ldots, \delta y_2\}$ are calculated from Eq. 25 and δS_w is calculated from Eq. 24. All $2N_c + 4$ unknowns then are updated as

$$P_{j,n+1} \cong P_j^{\ell+1} = P_j^{\ell} + \delta P_j \quad j = 1, 2, \ldots, N , \quad \ldots\ldots\ldots\ldots (27)$$

where a damping factor may be used on δP_j if iterate changes are excessive.

The values $P_j^{\ell+1}$ are used to re-evaluate terms in C, Υ, and $\underline{R}$ in Eq. 26, and that equation is solved

again. These iterations continue until max $|\delta P_j|$ over the grid are less than specified tolerances. We generally use 1 psi (6.89 kPa) for pressure, 0.01 for saturations, and 0.002 for mole fractions.

Variable Substitution

The above description of the model formulation treats the general case where both oil and gas phases are present. If no free gas is present, the $2N_c + 4$ model equations (Eqs. 1 through 5) become $N_c + 3$ equations in the $N_c + 3$ unknowns, $\{x_i\}, p, S_o, S_w$. The $N_c + 1$ deleted equations are the N_c fugacity constraints (Eq. 3) and the gas-phase mole fraction constraint (Eq. 4b). The corresponding $N_c + 1$ deleted unknowns are $\{y_i\}$ and S_g.

The $N_c + 3$ equations are expanded as described above as linear combinations of the $N_c + 3$ variables $\{\delta P_j\} = \{\delta x_1, \delta x_2, \ldots, \delta x_{N_c}, \delta p, \delta S_o, rS_w\}$. The set of $N_c + 1$ primary equations is obtained by eliminating δx_{N_c} using Eq. 23a and δS_w using Eq. 24, with $\delta S_g = S_g^{\ell} = 0$. The remaining set of $N_c + 1$ primary variables is $\{\delta x_1, \delta x_2, \ldots, \delta x_{N_c-1}, \delta p, \delta S_o\}$.

A similar variable substitution is performed for the case where oil saturation is zero. In any case, we always solve $N_c + 1$ simultaneous, primary equations in $N_c + 1$ unknowns by direct solution. In general, of course, adjacent grid blocks may have different sets of primary variables.

Case of Water Immobility

If water is present but immobile throughout the reservoir, the right side of the water mass balance (Eq. 2) is zero and that equation may be treated as a constraint equation as opposed to a primary equation. This reduction from $N_c + 1$ to N_c primary equations can be important since the computing time associated with direct solution of n simultaneous equations[18] is proportional to n^3.

If water is immobile, the model formulation is as described above with the following exception. The variable δS_w is eliminated from expanded Eq. 2 and constraint Eq. 24. The resulting equation in δS_o and δS_g is then used to eliminate δS_g from the N_c, expanded-component mass balance equation (Eq. 1). The resulting N_c primary variables then include only one saturation, δS_o, for the case where oil and gas phases are present and no saturations when oil or gas phase saturation is zero.

Hydrocarbon-Phase Appearance/Disappearance

The case of hydrocarbon-phase disappearance during a time step is quite simple. If both oil and gas phases are present in a grid block at the end of iteration ℓ, the solution $\{P_j\}^{\ell+1}$ includes $S_o^{\ell+1}$ and $S_g^{\ell+1}$. If either of these saturations is negative, it is set to zero before initiating the next iteration.

If S_o^{ℓ} or S_g^{ℓ} is zero in a grid block, then a saturation pressure calculation, described in the Appendix, is performed for the block's single-phase hydrocarbon fluid. If calculated p_s is less than the grid-block pressure p^{ℓ}, the block remains in single hydrocarbon-phase mode. If p_s exceeds p^{ℓ}, the absent-phase saturation is set to 0.001, for example, and the present hydrocarbon phase S^{ℓ} is decreased by 0.001. We apply this test each iteration. The saturation pressure calculation is not performed for two-phase (hydrocarbon) grid blocks.

Numerical Dispersion Controls

MCM calculations exhibit considerable numerical dispersion. One occurrence of this numerical dispersion is at the leading edge of the two-phase (gas/oil) displacement. The region downstream of this leading edge or gas saturation "shock" front should consist of oil at original composition.* With no control, the calculated oil composition is smeared appreciably downstream from this front. We effectively prevent this numerical dispersion by specifying oil outflow composition as *original* oil composition for each grid block until a gas phase appears in the block.

Discussion of Model Formulation

We summarize here some advantageous features of this formulation, which are absent from some or all of the earlier reported models.[1-7,12] The formulation is three-dimensional and treats flow of all three (gas, oil, and water) phases accounting for capillary and gravity as well as viscous forces. Hydrocarbon-phase relative permeability and capillary pressure are dependent on interfacial tension in addition to saturation.

The implicit nature of the formulation removes a time-step limitation associated with models using explicit transmissibilities. In that case, a single-phase (hydrocarbon) grid block cannot experience a throughput (volumetric flow in or out) larger than the phase's volume in place in the block. In some cross sections and/or single-well radial-z calculations, the corresponding time-step limitation can be severe.

The "price" paid by the implicit formulation for this tolerance of larger time steps is the increased arithmetic per time step required for simultaneous solution of $N_c + 1$ primary equations. As the number of components becomes larger, this penalty increases rapidly and must be offset by use of increasingly larger time steps. The developing use of vector or array processor hardware may reduce significantly the ratio of equation/solution to coefficient-generation time with a result more favorable to implicit than explicit formulations.

The formulation described here does not generate or use equilibrium K-values per se and requires no flash calculation. However, the fugacity constraints are entirely equivalent to the direct use of K-values as $y_i = K_i x_i$, and one iteration of the flash calculation automatically is incorporated or performed in each overall iteration for each two-phase grid block.

Fussell and Fussell[12] report selection of two different reduced sets of equations and iteration variables for a two-phase grid block, depending on whether the block is predominantly liquid or vapor.

*Physical dispersion or mechanical mixing actually will result in some smearing of oil composition at this front, but the mixed zone is small compared with that produced by numerical dispersion.

TABLE 1 – COMPARISON OF CALCULATED AND EXPERIMENTAL RESULTS RESULTS FOR THE METHANE/BUTANE/DECANE SYSTEM[19]

				K-value	
T(°F)	x_i	*p* (psia)	*p*, calculated (psia)	Experimental[19]	Calculated
280	$x_i = 0.203$	1,000	1,019.7	$K_1 = 3.813$	3.773
	$x_2 = 0.346$			$K_2 = 0.613$	0.637
	$x_3 = 0.451$			$K_3 = 0.032$	0.031
280	0.402	2,000	1,970.5	1.861	1.867
	0.370			0.605	0.613
	0.228			0.122	0.099
280	0.575	3,000	2,997.6	1.459	1.475
	0.179			0.631	0.635
	0.246			0.193	0.156
160	0.253	1,000	972.7	3.174	3.173
	0.661			0.297	0.297
	0.086			0.013	0.008
160	0.459	2,000	1,950.9	1.854	1.862
	0.390			0.367	0.361
	0.151			0.039	0.028
160	0.663	3,000	3,128.2	1.213	1.254
	0.229			0.703	0.633
	0.108			0.330	0.218

TABLE 2 – COMPARISON OF CALCULATED Ω_a AND Ω_b VALUES FOR METHANE, BUTANE, AND DECANE

	Ω_{ai}		Ω_{bi}	
Component	Ref. 12	This Work	Ref. 12	This Work
Methane	0.4251	0.42617	0.0859	0.086173
Butane	0.4154	0.419367	0.0759	0.0794
Decane	0.46512	0.451875	0.07259	0.070452

TABLE 3 – MODEL DATA FOR RUNS 1 THROUGH 3

Reservoir length, ft	250
Width, ft	100
Thickness, ft	50
Permeability, md	2,000
Porosity	0.2
c_w, psi^{-1}	0.000003
c_r, psi^{-1}	0.000004
One-dimensional grid, blocks	80, 40, 20 (Runs 1, 2, 3)
Capillary pressure	0
Relative permeability data	
S_{wc}	0.2
S_{org}	0.2
S_{gc}	0
S_{gr}	0.15
k_{rocw}	1.0
k_{rgcw}	1.0
k_{rw}	0
$n_{og} = n_g$	2 (see Eqs. A-29 and A-30)
Initial pressure, psia	2,000
Reservoir temperature, °F	160
Initial saturations	
S_w, S_o, S_g	0.2, 0.8, 0
Initial oil composition	
x_1, x_2, x_3	0.2, 0.2, 0.6
Initial calculated oil viscosity[15], cp	1.07
Stock-tank conditions, psia, °F	14.7, 60

100 Mcf/D of 68.4 mol% methane, 31.6 mol% butane injected at $x = 0$.
Production at $x = 250$ ft on deliverability at 2,000 psia.

Our formulation uses a fixed set of reduced (primary) equations and variables for saturations $0 < S_g < 1.0$.

The use of an equation of state, together with use of equation of state densities in the Lohrenz *et al.* viscosity calculation,[15] ensures smooth convergence of phase compositions and all properties to critical point values as the latter is approached.

Applications

In applications to date, we have experienced little difficulty and few "surprises" in simulating depletion or cycling operations. However, we have faced numerical dispersion and convergence problems in testing the model with the MCM type of problem. We are satisfied with the convergence attained by the implicit formulation described above but feel that numerical dispersion deserves further attention and attempts at control.

The applications described here include one- and two-dimensional (cross-sectional) example problems. Water is present but immobile in all calculations. The methane/butane/decane system is used for the reservoir hydrocarbon content. Reservoir temperature is 160°F (344.3 K) for all calculations. Methane, butane, and decane are referred to hereafter as Components 1, 2, and 3, respectively.

As described in the Appendix, the modified Redlich-Kwong equation of state[14] requires values for parameters Ω_{ai} and Ω_{bi} for each component and binary interaction coefficient C_{ij}. We calculated Ω_{ai} and Ω_{bi} as described in the Appendix. Binary interaction coefficients $C_{ij} = 0$, except for $C_{12} = 0.024$ and $C_{23} = 0.025$, which were obtained from Zudkevitch and Joffe.[14]

Table 1 lists reported[19] experimental data for the methane/butane/decane system and presents a comparison with our calculated saturation pressures and *K*-values using the above mentioned Ω_a, Ω_b, and C_{ij} values. Zudkevitch and Joffe reported agreement between calculated and experimental results generally

comparable with that shown in Table 1. However, their agreement was exact in regard to pressure and their calculated decane K-values were better at 2,000 and 3,000 psia (13 789 and 20 684.3 kPa). Their unreported Ω_{ai} and Ω_{bi} values were undoubtedly somewhat different from ours, since we use a somewhat different procedure to calculate them. However, Fussell and Fussell[12] imply their use of Zudkevitch and Joffe's procedure and the former give the Ω_{ai} and Ω_{bi} values shown in Table 2. We used these values from Ref. 12 and obtained no improvement in match of pressure or K-values.

The single-cell calculation described in the Appendix was used to calculate the critical point composition at 2,000 psia (13 789.5 kPa) as $x_1 = 0.664$, $x_2 = 0.332$, and $x_3 = 0.004$. The same calculation was used to determine a methane/butane composition necessary to generate MCM in a horizontal, one-dimensional displacement. An injected composition of $y_1 = 0.684$ and $y_2 = 0.316$ was found to force the initial oil ($x_1 = 0.2$, $x_2 = 0.2$, and $x_3 = 0.6$) exactly to the critical point. A leaner injection gas gave calculated oil disappearance with a disparity in phase compositions, while a richer mixture gave either outright miscibility or a temporary gas phase that disappeared with disparity between phase compositions.

All fluid compositions mentioned here are mole fraction, not weight fraction.

One-Dimensional MCM Problem

Model Runs 1, 2, and 3 treat injection of a 68.4% methane/31.6% butane gas mixture into a linear reservoir with 20% water saturation and 80% undersaturated oil saturation. Oil composition was 20% methane, 20% butane, and 60% decane. Initial bubble-point and reservoir pressures were 821 psia (5660.6 kPa) and 2,000 psia (13 789.5 kPa), respectively. Initial oil in place, calculated by flashing the oil at stock-tank conditions of 14.7 psia (101.4 kPa) and 60°F (101.4 K) was 35,342 STB (5619 stock-tank m^3), and stock-tank GOR was 267 scf/STB (42 std m^3/stock-tank m^3).

The reservoir dimensions, permeability, porosity, and other input data are listed in Table 3. Gas injected was 100 Mcf/D (2831.7 m^3/d), and production was on deliverability against a flowing bottomhole pressure of 2,000 psia (13 789.5 kPa).

Runs 1, 2, and 3 were performed with specified, constant time steps of 1.875, 3.75, and 7.5 days, respectively, so that the ratio time-step/cell-volume was the same for all runs. The resulting maximum (over grid) changes in saturation and mole fraction per time step were generally each less than 0.1. However, at steps when phases converged to critical composition, saturation change per step was as high as 0.50.

Runs, 1, 2, and 3 were performed using 80, 40, and 20 grid blocks, respectively. Fig. 1 shows calculated gas saturation profiles vs. distance at 210 days for the three runs. This figure shows a considerable effect of numerical dispersion on the rate of advance of the miscible front. The two-phase gas/oil zone

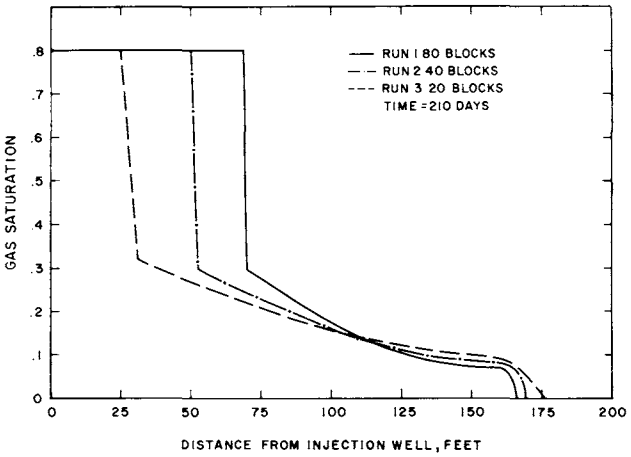

Fig. 1 – Calculated gas saturation vs. distance.

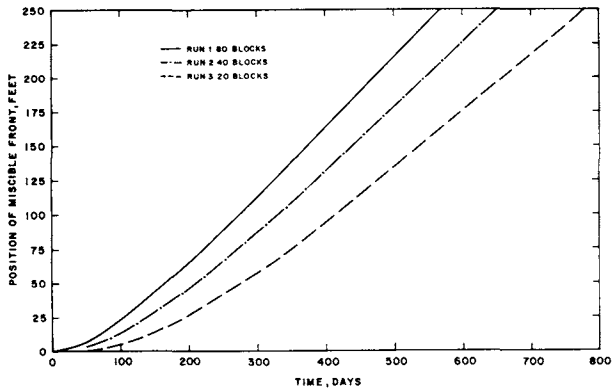

Fig. 2 – Calculated miscible-front advance vs. time.

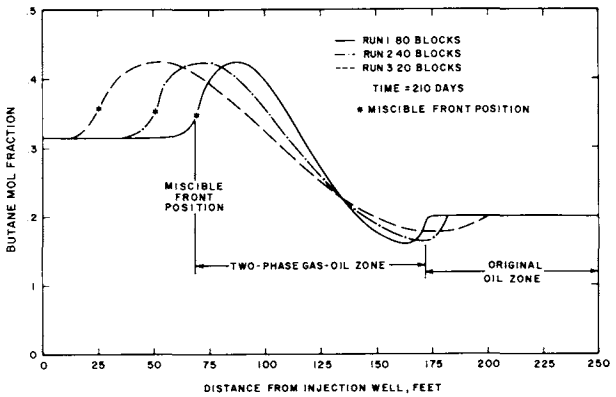

Fig. 3 – Calculated butane mole fraction vs. distance.

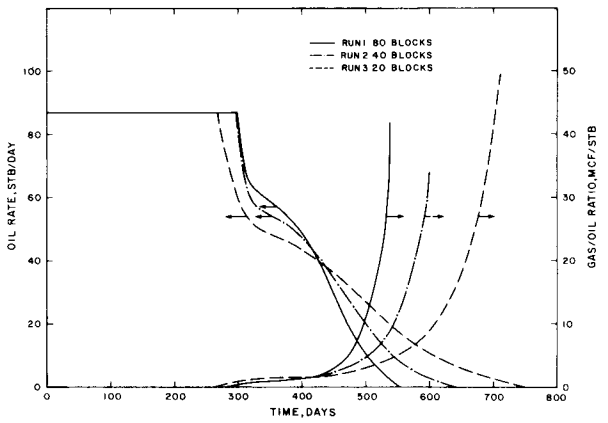

Fig. 4 – Calculated oil production rate and GOR vs. time.

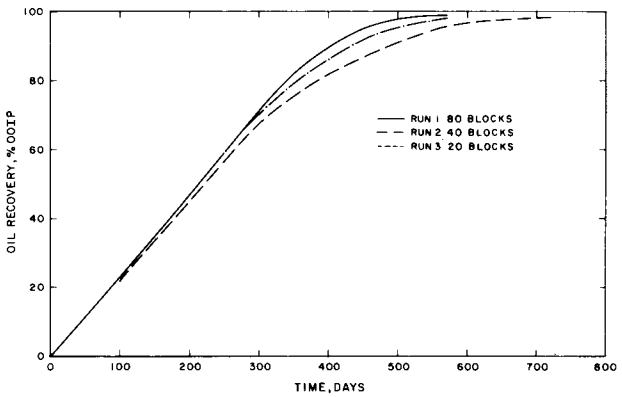

Fig. 5 – Calculated oil recovery vs. time.

saturations are less sensitive to number of grid blocks. Fig. 2 further illustrates the increase in calculated miscible-front velocity with an increasing number of grid blocks.

Fig. 3 shows calculated butane (intermediate component) mole fraction vs. distance at 210 days. Initial butane mole fraction was 0.2 and injected butane mole fraction was 0.316. The calculations indicate an upstream miscible zone of injected gas composition, a two-phase zone of variable composition, and a final, downstream, single-phase oil zone of original oil composition. Actually, the downstream or leading portion of the two-phase zone should be a plateau of constant composition, but its existence is masked by numerical dispersion effects. This plateau can be proved by the analytical solution technique of Welge *et al.*[20] and is discussed by other authors.[6,7] Fig. 3 again shows that numerical dispersion is more pronounced in the vicinity of the miscible front than in the two-phase zone.

Fig. 4 shows the effect of grid block size on calculated oil rate and surface GOR vs. time. Finally, Fig. 5 shows cumulative oil recovery vs. time.

In all these runs, a given grid block progressed in time from original oil composition to a two-phase (gas/oil) configuration and finally to a single-phase (miscible) mode. The gas- and oil-phase compositions during the two-phase period continuously converged toward critical composition. The two-phase to single-phase transition occurred due to phase convergence – i.e., convergence of both phase compositions to critical composition – rather than oil or gas phase disappearance with a phase composition disparity.

Of these results, perhaps the least sensitive to effects of numerical dispersion is calculated cumulative oil recovery vs. time. However, the 80-block Run 1 is not the "correct" answer in that it still displays numerical dispersion effects. Other authors[6,9] presenting one-dimensional MCM numerical calculations mention use of 100 and up to 300 grid blocks. Elimination or significant reduction of numerical dispersion in 10 to 20 grid-block representations obviously requires control measures undiscovered in this study. Attempts to analyze and control this dispersion are discussed by several authors.[6,7,21]

Welge *et al.*[20] report that their analytical solution for this type of problem shows that saturation and composition profiles are unique but simply "stretch" with time. This implies that use of grid block size increasing with distance from the injection well might reduce space truncation error using a fixed total number of cells. This idea was in effect used in an earlier study,[7] where grid block size was increased in groups from injector to producer. We repeated the 20-block Run 3 with $\Delta x_i = \alpha \Delta x_{i-1}$ and $\alpha = 1.15$ so that Δx_1 was 2.44 ft (0.7437 m) and Δx_{20} was 34.73 ft (10.6 m). Compared with the constant-Δx Run 3, agreement with the 80-block run was better at early time but worse at later time.

Two-Dimensional, Gas-Injection Runs

Cross-sectional x-z Runs 4 through 7 were performed for gas injection into a highly stratified reservoir. We examined the effect on calculated oil recovery of permeable zone ordering, k_v/k_H ratio, and injection-gas composition. The example reservoir is 400 ft (121.9 m) long, 100 ft (30.48 m) wide, 80 ft (24.38 m) thick, and is represented by a 20 × 4 grid. Permeability of the four layers varies from 20 to 2,500 md. Initial oil saturation, pressure, and composition are identical to those used in the one-dimensional Runs 1 through 3. Model input data different from or additional to those given in Table 3 are given in Table 4. Initial oil in place was 95,007 STB (15 105 stock-tank m^3).

In Runs 4 through 6, injection gas of 68.4 mol% methane and 31.6 mol% butane was injected at 100 Mcf/D (2831.7 m^3/d) into all four layers in proportion to layer permeability/thickness product. The production well was completed in all four layers and produced on deliverability against a 2,000-psia (13 789.5 kPa) flowing bottomhole pressure.

For Run 4, permeabilities were 20, 100, 500, and 2,500 md in Layers 1, 2, 3, and 4 (top to bottom), respectively, and the k_v/k_H ratio was 1.0. The only change for Run 5 was reduction of k_v/k_H to 0.1. Run 6 had a k_v/k_H of 1.0, but the layer ordering was reversed with Layer 1 through 4 permeabilities of

2,500, 500, 100, and 20 md, respectively.

Runs 4 through 7 were performed using automatic time steps controlled by maximum grid block changes (per time step, over entire grid) of 0.15 for both saturations and mole fractions.

The effect of the 10-fold reduction in k_v/k_H was very little. The times of free-gas appearance or breakthrough at the production well in Layers 1 through 4 in Run 4 were 628, 900, 1,020, and 1,620 days, respectively. The corresponding times for Run 5 were 870, 745, 990, and 1,350 days. Thus, gas broke through most rapidly in Layer 1 for Run 4 but in Layer 2 for Run 5. In spite of the pronounced permeability increase with depth, Run 4 indicated a rather strong gas override. When free gas broke through in Layer 1, the free-gas fronts in Layers 2, 3, and 4 were advanced only 65, 55, and 15%, respectively, of the distance from injector to producer. In Runs 4 and 5, only a very limited miscible zone was present at 2,160 days. This zone existed only in Layer 3, a distance of about 30% of reservoir length from the injector.

Fig. 6 compares calculated oil recovery and GOR vs. time for Runs 4 and 6. In Run 6, free gas broke through at the producer in Layer 1 at 262 days and in Layer 2 at 1,338 days. The high permeability at the formation top in Run 6 aggravated the gas override and reduced oil recovery from more than 90 to 53% of original oil in place. In Run 6, the miscible zone existed only in Layer 1 and broke through at the producer at 1,570 days. While this miscible zone initially appeared with phase convergence at critical composition, the gas composition subsequently became leaner than the injected composition due to percolation or upward flow from Layer 2 of leaner, immiscible (in Layer 2) gas. The calculated methane mole fraction of Layer 1 gas was uniformly 70% at 2,160 days.

Run 7 is the same as Run 4, with the permeable layer at the bottom and $k_v/k_H = 1$, but injection gas is a lean 90 mol% methane, 10 mol% butane. Fig. 7 shows that the lean gas injection gives somewhat higher early oil recovery, but gas overrides and breaks through quickly at 379 days in Layer 1 and 394 days in Layer 2. Calculated GOR rises rapidly and final recovery at 2,160 days is only 59% of original oil in place, compared with 91% recovery for Run 4 using richer gas injection.

This lean gas of Run 7 is very similar to an equilibrium gas in that its composition lies very close to the phase envelope. Thus, there is not a pronounced vaporization or condensation mechanism and no calculated oil saturation anywhere in the reservoir is reduced below 0.18. This "immiscible" character of the injected gas explains the early higher oil recovery (than Run 4), which is caused directly by slightly higher reservoir pressurization early in Run 7.

Efficiency of the Formulation

Computing time required for a formulation is of interest since comparison of overall efficiencies of different formulations is helpful in continuing

TABLE 4 – MODEL DATA FOR TWO-DIMENSIONAL RUNS 4 THROUGH 7

Reservoir length: 400 ft
Reservoir width: 100 ft

Layer	k (md)	ϕ	PI (res bbl-cp/D-psi)
1	20	0.18	2
2	100	0.20	10
3	500	0.22	50
4	2500	0.24	250

Layers were reversed in order for Run 6.
$k_v/k_H = 1.0$ except for 0.1 value used in Run 5.
Vertical permeability is calculated as harmonic average of adjacent layer permeabilities.
$P_{cgo} = 20\,S_g^3$.
Injection = 100 Mcf/D of 68.4% methane, 31.6% butane, Runs 4 through 6.
= 100 Mcf/D of 90% methane, 10% butane, Run 7.
Production at $x = 400$ ft from all four layers on deliverability at 2,000 psia opposite center of top layer.

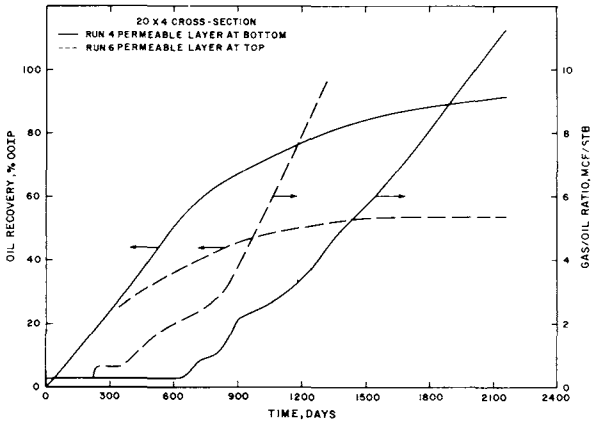

Fig. 6 – Calculated oil recovery and GOR.

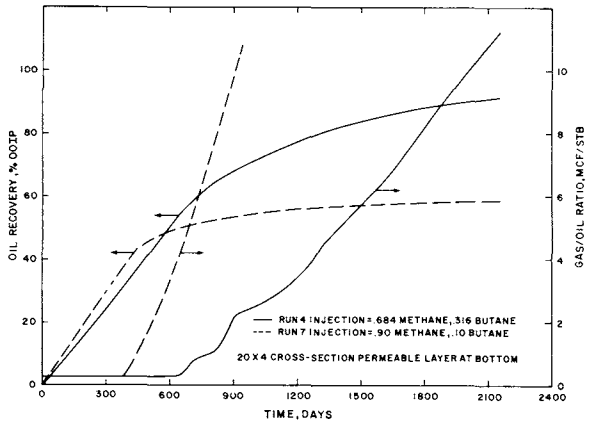

Fig. 7 – Calculated oil recovery and GOR.

development efforts. All computing times mentioned here are CDC 6600 CPU seconds. One-dimensional Runs 1, 2, and 3 required 0.036 second per block step for total run times of 872, 239, and 75 seconds, respectively. Average iterations per time step for each run was about 3.25.

Two-dimensional Runs 4 through 7 were carried out to 2,160 days. Run 4 required the most computing time, 474 seconds for 114 steps and 465 iterations, or an average of 4.08 iterations per time step. Computing time per block step was 0.052 second.

Fussell and Fussell[12] reported a computing time requirement of 0.0066 to 0.0254 (CDC 6600) seconds per block step for a three-component problem for their semi-implicit equation of state compositional model. They actually reported IBM 370/168 times, and we use a factor of 2.2 for CDC 6600 time/IBM 370/168 time. They reported calculated results for immiscible gas injection in a 13 × 9 cross section, using the methane/butane/decane system but did not give time step or overall computing time information.

We performed an 11 × 9 cross-sectional run similar to their example to determine the increased computing time requirement of this formulation due to an increase in bandwidth from four (in Runs 4 through 7) to nine. The computing time per block per iteration increased only from 0.0128 to 0.0159 second. The 1,080-day run required 14 time steps and 115 seconds and corresponds to 0.375 HPV injected.

Summary

An implicit formulation using an equation of state has been described for simulation of multidimensional, compositional problems. Applicability of the formulation ranges from cycling or depletion of volatile oil and gas condensate reservoirs to outright or multicontact miscible flooding operations.

Computational testing with example problems indicates stable convergence of this formulation as hydrocarbon-phase compositions and properties converge near a critical point. Continuing effort is directed toward comparison of model results with laboratory results for both MCM and outright-miscibility cases.

The reported computational testing centered on the MCM process since ability to stably and efficiently compute behavior very close to a critical point is perhaps the most severe test of a compositional formulation. Our example-problem results for this process indicate significant numerical dispersion primarily affecting the calculated velocity of miscible-front advance. Further effort is required to analyze and reduce this numerical dispersion.

While we report detailed problem descriptions, results, and associated computing times, we lack similar reported times necessary to assess the relative overall efficiency of an implicit formulation as opposed to semi-implicit formulations.

Nomenclature

c_r = rock compressibility, 1/psi (1/kPa)
c_w = water compressibility, 1/psi (1/kPa)
C_{ij} = modified Redlich-Kwong equation binary interaction coefficients
f = fugacity, psia (kPa)
f_i = fugacity of Component i in a mixture
k = permeability, md
k_H = horizontal permeability
k_r = relative permeability, fraction
k_{rgcw} = relative permeability to gas at connate water
k_{rocw} = relative permeability to oil at connate water
k_v = vertical permeability
K_i = equilibrium K-value for Component i, y_i/x_i
n_w, n_{ow}, n_{og}, n_g = exponents on relative permeability curves
N = $2N_c + 4$
N_c = number of hydrocarbon components
p = gas-phase pressure
p_o = original reservoir pressure
p_s = saturation pressure
P_{cgo} = gas/oil capillary pressure, $p_g - p_o$, psi (kPa)
P_{chi} = parachor of Component i
P_{cwo} = water/oil capillary pressure, $p_o - p_w$, psi (kPa)
P_i = unknowns, see Eq. 6
PI_k = Layer k productivity index, cu ft-cp/D-psi (m^3)
q_i = production rate of Component i from grid block, mol/D
q_w = water production rate, mol/D
R = universal gas constant, 1.98 Btu/lbm mol − °R (J/mol·K)
S = phase saturation, fraction
S_{gc} = critical gas saturation
S_{gr} = residual gas saturation
S_{org} = residual oil saturation to gas
S_{orw} = residual oil saturation to water
S_{wir} = irreducible water saturation
t = time, days
Δt = time step, days
T = temperature, °R (K)
V = grid block volume, $\Delta x\ \Delta y\ \Delta z$, cu ft ($m^3$)
$\underline{V}$ = specific volume, cu ft/lbm mol (m^3/mol)
x_i = mole fraction of Component i in oil phase
$\Delta x, \Delta y, \Delta z$ = grid block dimensions, ft (m)
y_i = mole fraction of Component i in gas phase
z = subsea depth, measured positively downward, ft (m)
Z_k = depth to center of Layer k, ft (m)

γ = specific weight, psi/ft (kPa/m)
λ = phase mobility, k_r/μ
μ = viscosity, cp (Pa·s)
ρ = density, mol/cu ft (mol/m^3)
σ = interfacial tension, dynes/cm (mN/m)
Υ = fluid flow transmissibility, kA/L, reservoir cu ft-cp/D-psi (m^3)
ϕ = porosity, fraction, $\phi_o[1 + C_r(p - p_o)]$
ψ_i = fugacity coefficient of Component i, $f_i/p x_i$
ω = acentric factor
Ω_a, Ω_b = Redlich-Kwong equation parameters

Superscripts

ℓ = iteration number
L = hydrocarbon liquid phase
o = original
V = hydrocarbon gas phase

Subscripts

c = critical
g = gas
H = heavy hydrocarbon component
i = component
i,j,k = grid block indices in x, y, and z directions
L = hydrocarbon liquid phase
n = time step level
o = oil
s = saturated condition
w = water
wb = wellbore
V = gas phase
1,2 = adjacent Grid Blocks 1 and 2

Difference Notation

X is any quantity or arithmetic expression.

$\Delta X = X_1 - X_2$, where Subscripts 1 and 2 refer to adjacent Grid Blocks 1 and 2.

$$\Delta(\Upsilon\Delta X) \equiv \Delta_x(\Upsilon_x\Delta_x X) + \Delta_y(\Upsilon_y\Delta_y X) + \Delta_z(\Upsilon_z\Delta_z X),$$

and

$$\Delta_x(\Upsilon_x\Delta_x X) \equiv \Upsilon_{x,i+\frac{1}{2}}(X_{i+1} - X_i) - \Upsilon_{x,i-\frac{1}{2}}(X_i - X_{i-1}),$$

where $\Upsilon_{x,i+\frac{1}{2}}$ is x-direction transmissibility for flow between Grid Blocks i and $i+1$ and X_i is the value of X at Grid Block i. Subscripts j and k are suppressed here.

References

1. Price, H.S. and Donohue, D.A.T.: "Isothermal Displacement Processes With Interphase Mass Transfer," *Soc. Pet. Eng. J.* (June 1967) 205-320; *Trans.*, AIME, **240**.
2. Roebuck, I.F. Jr., Henderson, G.E., Douglas, Jim Jr., and Ford, W.T.: "The Compositional Reservoir Simulator: Case 1 – The Linear Model," *Soc. Pet. Eng. J.* (March 1969) 115-130; *Trans.*, AIME, **246**.
3. Culham, W.E., Farouq Ali, S.M., and Stahl, C.D.: "Experimental and Numerical Simulation of Two-Phase Flow With Interphase Mass Transfer in One and Two Dimensions," *Soc. Pet. Eng. J.* (Sept. 1969) 323-337; *Trans.*, AIME, **246**.
4. Kniazeff, V.J. and Naville, S.A.: "Two-Phase Flow of Volatile Hydrocarbons," *Soc. Pet. Eng. J.* (March 1965) 37-44; *Trans.*, AIME, **234**.
5. Nolen, J.S.: "Numerical Simulation of Compositional Phenomena in Petroleum Reservoirs," Reprint Series No. 11 – *Numerical Simulation*, Society of Petroleum Engineers, Dallas (1973) 269-284.
6. Van Quy, N., Simandoux, P., and Corteville, J.: "A Numerical Study of Diphasic Multicomponent Flow," *Soc. Pet. Eng. J.* (April 1972) 171-184; *Trans.*, AIME, **253**.
7. Corteville, J., Van Quy, N., and Simandoux, P.: "A Numerical and Experimental Study of Miscible or Immiscible Fluid Flow in Porous Media with Interphase Mass Transfer," paper SPE 3481 presented at the SPE 46th Annual Meeting, New Orleans, Oct. 3-6, 1971.
8. Metcalfe, R.S., Fussell, D.D., and Shelton, J.L.: "A Multicell Equilibrium Separation Model for the Study of Multiple Contact Miscibility in Rich-Gas Drives," *Soc. Pet. Eng. J.* (June 1973) 147-155; *Trans.*, AIME, **255**.
9. Fussell, D.D., Shelton, J.L., and Griffith, J.D.: "Effect of 'Rich' Gas Composition on Multiple-Contact Miscible Displacement – A Cell-to-Cell Flash Model Study," *Soc. Pet. Eng. J.* (Dec. 1976) 310-316; *Trans.*, AIME, **261**.
10. Cook, Alton B., Walter, C.J., and Spencer, George C.: "Realistic K-Values of C_{7+} Hydrocarbons for Calculating Oil Vaporization During Gas Cycling at High Pressure," *J. Pet. Tech.* (July 1969) 901-915; *Trans.*, AIME, **246**.
11. Fussell, D.D. and Yanosik, J.L.: "An Iterative Sequence for Phase Equilibria Calculations Incorporating the Redlich-Kwong Equation of State," *Soc. Pet. Eng. J.* (June 1978) 173-182.
12. Fussell, L.T. and Fussell, D.D.: "An Iterative Technique for Compositional Reservoir Models," *Soc. Pet. Eng. J.* (Aug. 1979) 211-220.
13. Redlich, O. and Kwong, J.N.S.: "On the Thermodynamics of Solutions. V. An Equation of State. Fugacities of Gaseous Solutions," *Chem. Rev.* (1949) **44**, 233.
14. Zudkevitch, David and Joffe, Joseph: "Correlation and Prediction of Vapor-Liquid Equilibria with the Redlich-Kwong Equation of State," *AIChE J.* (Jan. 1970) **16**, No. 1, 112-119.
15. Lohrenz, J., Bray, B.G., and Clark, C.R.: "Calculating Viscosity of Reservoir Fluids From Their Composition," *J. Pet. Tech.* (Oct. 1964) 1171-1176; *Trans.*, AIME, **231**.
16. Reid, R.C. and Sherwood, T.K.: *The Properties of Gases and Liquids*, Third ed., McGraw-Hill Book Co. Inc., New York City (1977).
17. Price, H.S. and Coats, K.H.: "Direct Methods in Reservoir Simulation," *Soc. Pet. Eng. J.* (June 1974) 295-308; *Trans.*, AIME, **257**.
18. Coats, K.H.: "A Highly Implicit Steamflood Model," *Soc. Pet. Eng. J.* (Oct. 1978) 369-383.
19. Reamer, H.H., Fiskin, J.M., and Sage, B.H.: "Phase Equilibria in Hydrocarbon Systems: Phase Behavior in the Methane-n-Butane-Decane System at 160°F," *Ind. Eng. Chem.* (Dec. 1949) **41**, 2871-2875.
20. Welge, H.J., Johnson, E.F., Ewing, S.P., and Brinkman, F.H.: "The Linear Displacement of Oil from Porous Media by Enriched Gas," *J. Pet. Tech.* (Aug. 1961) 787-796; *Trans.*, AIME, **222**.
21. Camy, J.P. and Emanuel, A.S.: "Effect of Grid Size in the Compositional Simulation of CO_2 Injection," paper SPE 6894 presented at the SPE Annual Technical Conference and Exhibition, Denver, Oct. 9-12, 1977.
22. Yarborough, L.: "Application of a Generalized Equation of State to Petroleum Reservoir Fluids," paper presented at the Symposium of Equations of State in Engineering and Research, 176th ACS National Meeting, Miami Beach, FL, Sept. 10-15, 1978.
23. Coats, K.H.: "In-Situ Combustion Model," paper SPE 8394 presented at the SPE 54th Annual Technical Conference and Exhibition, Las Vegas, Sept. 23-26, 1979.
24. Stone, H.L.: "Estimation of Three-Phase Relative Permeability and Residual Oil Data," *J. Cdn. Pet. Tech.* (Oct.-Dec. 1973) 53-61.

25. Peng, D.Y. and Robinson, D.B.: "A Rigorous Method for Predicting the Critical Properties of Multicomponent Systems from an Equation of State," *AIChE J.* (1977) **23**, 137-144.
26. Baker, Lee E. and Kraemer, P.L.: "Critical Point and Saturation Pressure Calculations for Multicomponent Systems," *Soc. Pet. Eng. J.* (Feb. 1980) 15-24.

APPENDIX

PVT Treatment

Hydrocarbon liquid- and gas-phase densities and component fugacities are computed from the Redlich-Kwong equation of state[13] in a modified form nearly identical to that described by Zudkevitch and Joffe.[14] A recent paper by Yarborough[22] discusses this modified equation and presents detailed results of its application to reservoir fluids. In part, he provides a number of binary interaction coefficients for this equation of interest in reservoir work.

The modified equation is

$$p = \frac{RT}{\underline{V}-b} - \frac{a}{T^{0.5}\underline{V}(\underline{V}+b)} , \quad \text{(A-1)}$$

where, for a liquid-phase mixture,

$$a = \sum_{i=1}^{N}\sum_{j=1}^{N} x_i x_j a_{ij} , \quad \text{(A-2)}$$

$$a_{ij} = (1-C_{ij})(a_i a_j)^{0.5} , \quad \text{(A-3)}$$

$$a_i = \Omega_{ai} R^2 T_{ci}^{2.5}/p_{ci} , \quad \text{(A-4)}$$

$$b = \Sigma x_i b_i , \quad \text{(A-5)}$$

$$b_i = \Omega_{bi} R\, T_{ci}/p_{ci} , \quad \text{(A-6)}$$

and C_{ij} = binary interaction coefficient.

For a gas-phase mixture, y_i are used in place of x_i in Eqs. A-2 and A-5. Eq. A-1 can be written in terms of compressibility factor as

$$z^3 - z^2 + (A - B^2 - B)z - AB = 0 , \quad \text{(A-7)}$$

where

$$A = ap/R^2 T^{2.5} , \quad \text{(A-8)}$$

and

$$B = bp/RT . \quad \text{(A-9)}$$

The fugacity coefficient of Component i in a mixture is $\psi_i \equiv f_i/px_i$ and is defined by[16]

$$RT \ln \psi_i = -\int_{\infty}^{V} \left(\frac{\partial p}{\partial N_i} - \frac{RT}{V}\right) dV - RT \ln z , \quad \text{(A-10)}$$

where V here is total volume of N mixture moles and N_i is moles of Component i in the mixture.

Using Eq. A-1 in Eq. A-10 gives

$$\frac{f_i}{px_i} = \psi_i = \frac{1}{z-B}\left(\frac{z+B}{B}\right)^{E_i} e^{\frac{B_i}{B}(z-1)} , \quad \text{(A-11)}$$

where

$$E_i = \frac{A}{B}\left(\frac{B_i}{B} - \frac{2}{A}\sum_{j=1}^{N} x_j A_{ij}\right), \quad \text{(A-12)}$$

$$A_{ij} = a_{ij}\, p/R^2 T^{2.5} , \quad \text{(A-13)}$$

and

$$B_i = b_i\, p/RT . \quad \text{(A-14)}$$

The expression (Eq. A-11) for component fugacity is derived or given by a number of authors.[11-14]

Eqs. A-7 and A-11 apply separately to the liquid and gas hydrocarbon phases with mole fractions $\{x_i\}$ and $\{y_i\}$ used, respectively, in calculating A, B, and other composition-dependent terms. In Eq. A-11, z_L or z_G is used when the equation is applied to the liquid or gas phase, respectively.

For the unmodified Redlich-Kwong equation,[13] $\Omega_a = 0.4274802327$ and $\Omega_b = 0.08664035$ and are independent of temperature, pressure, composition, and particular component. Zudkevitch and Joffe[14] calculate Ω_{ai} and Ω_{bi} for each Component i at a given temperature using the component's saturation pressure, saturated liquid density, and Lyckman's fugacity coefficient.

We calculate Ω_{ai} and Ω_{bi} at any temperature from the two equations

$$f_i^L = f_i^V , \quad \text{(A-15)}$$

and

$$z^L = z_i^* , \quad \text{(A-16)}$$

where z_i^* is the saturated liquid z factor of the component and pressure is specified as the saturation pressure at the given temperature. Eqs. A-15 and A-16, therefore, are two equations in the two unknowns Ω_{ai} and Ω_{bi} and are solved using the Newton-Raphson method.

Results described in this paper were obtained using Reidel's vapor-pressure equation[16] and Gunn and Yamada's method[16] to obtain saturated pressures and liquid densities.

If the temperature T is above T_c for the component, we use critical properties to determine Ω_{ai} and Ω_{bi}, as suggested by Zudkevitch and Joffe. We use z_{ci} and their suggested critical fugacity,

$$\log \psi_{ci} = -0.1754 - 0.0361\, \omega_i , \quad \text{(A-17)}$$

where ω_i is the Component i acentric factor. Thus, the two equations for determining Ω_{ai} and Ω_{bi} for $T > T_c$ are

$$\psi^L(A,B) - \psi_{ci} = 0 , \quad \text{(A-18a)}$$

and

$$z(A,B) - z_{ci} = 0 , \quad \text{(A-18b)}$$

with $T = T_c$ and $p = p_c$.

Phase Density Calculation

Hydrocarbon liquid- and gas-phase densities are calculated as

$$\rho = p/zRT, \quad \text{(A-19)}$$

where z is obtained from the latest iterate phase composition and pressure values by solution of Eq.

A-7 using the analytical solution for a cubic equation. Derivatives of ρ_o with respect to $\{x_i\}$ and pressure are obtained as

$$\frac{\partial \rho_o}{\partial p} = \left(1 - \frac{1}{z_L}\frac{\partial z_L}{\partial p}\right)\Big/ z_L RT, \quad \ldots\ldots\ldots (A\text{-}20)$$

and

$$\frac{\partial \rho_o}{\partial x_i} = -\frac{p}{z_L^2 RT}\frac{\partial z_L}{\partial x_i}, \quad \ldots\ldots\ldots\ldots\ldots (A\text{-}21)$$

where Eq. A-7 gives

$$\frac{\partial z_L}{\partial p} = \frac{\partial z_L}{\partial A}\frac{\partial A}{\partial p} + \frac{\partial z_L}{\partial B}\frac{\partial B}{\partial p} \quad \ldots\ldots\ldots\ldots (A\text{-}22)$$

and

$$\frac{\partial z_L}{\partial x_i} = \frac{\partial z_L}{\partial A}\frac{\partial A}{\partial x_i} + \frac{\partial z_L}{\partial B}\frac{\partial B}{\partial x_i} \quad \ldots\ldots\ldots (A\text{-}23)$$

plus

$$\frac{\partial z_L}{\partial A} = \left(B - z_L\right)\Big/\left(3z_L^2 - 2z_2 + A - B^2 - B\right) \ldots (A\text{-}24)$$

and

$$\frac{\partial z_L}{\partial B} = \left[A + (2B+1)z_L\right]\Big/\left(3z_L^2 - 2z_L + A - B^2 - B\right). \quad \ldots\ldots\ldots\ldots (A\text{-}25)$$

The derivatives $\partial A/\partial p$, $\partial A/\partial x_i$, etc., are calculated from Eqs. A-2 through A-6, A-8, and A-9. Calculation of gas-phase density derivatives is identical except that z_V and $\{y_i\}$ replace z_L and $\{x_i\}$.

Saturation Pressure Calculation

Saturation pressure is calculated in the manner proposed by Fussell and Yanosik,[11] with one minor exception. They propose solution of the $N_c + 1$ equations,

$$f_i^L - f_i^V = 0, \quad i = 1,2,\ldots,N_c \quad \ldots\ldots\ldots (A\text{-}26)$$

and

$$p_s - \sum_{j=1}^{N_c} \frac{f_j^L}{\psi_j^V} = 0, \quad \ldots\ldots\ldots\ldots\ldots (A\text{-}27)$$

for the $N_c + 1$ unknowns $\{y_1, y_2, \ldots, y_{N_c}, p_s\}$ using the Newton-Raphson method to obtain saturation pressure of a liquid phase. We have found somewhat improved convergence by replacing Eq. A-27 with

$$\sum_{j=1}^{N_c} y_i = 1.0. \quad \ldots\ldots\ldots\ldots\ldots\ldots (A\text{-}28)$$

This saturation pressure calculation is performed each iteration for each grid block where $S_g = 0$ or $S_o = 0$. The recalculated saturation pressure and absent phase composition are stored and used as starting values for the next iteration's Newton-Raphson solution of Eqs. A-26 and A-28.

Fugacity Calculation

Hydrocarbon liquid- and gas-phase component fugacities and their derivatives are calculated each iteration for all three-phase (including water) grid blocks from Eqs. A-11 and A-7 using latest iterate values of composition and pressure. The phase z factor is first calculated from Eq. A-7 along with derivatives of z with respect to composition and pressure.

Relative Permeability

Analytical representations for individual-phase relative permeabilities are used here in describing the relative permeability calculations. The model has the option of reading tabular data in lieu of the analytical forms. k_{rw} and k_{row} denote relative permeabilities to water and oil, respectively, measured in a core containing no free gas. k_{rog} and k_{rg} are relative permeabilities to oil and gas measured in the core containing irreducible water saturation.

Under immiscible conditions, gas/oil relative permeability curves generally exhibit considerable curvature, and residual gas and residual oil saturations below which the respective phases are immobile. Near a critical point, however, interfacial tension approaches zero, residual phase saturations decrease toward zero, and the relative permeability curves must approach straight lines. The treatment give here is not based on any theory or experimental evidence; it is simply devised to exhibit the described behavior with interfacial tension reduction.

The two-phase gas and oil curves used in this work are

$$k_{rg} = k_{rgcw}\left\{f(\sigma)\bar{S}_g^{\,n_g} + \left[1 - f(\sigma)\right]\bar{S}_g\right\} \quad \ldots (A\text{-}29)$$

and

$$k_{rog} = f(\sigma)\bar{S}_o^{\,n_{o_g}} + \left[1 - f(\sigma)\right]\bar{S}_o, \quad \ldots\ldots (A\text{-}30)$$

where

$$\bar{S}_g = \frac{S_g - S_{gr}^*}{1 - S_{wir} - S_{gr}^*}, \quad \ldots\ldots\ldots\ldots (A\text{-}31)$$

$$\bar{S}_o = \frac{1 - S_g - S_{wir} - S_{org}^*}{1 - S_{wir} - S_{org}^*}, \quad \ldots\ldots\ldots\ldots (A\text{-}32)$$

and

$$f(\sigma) = \left(\frac{\sigma}{\sigma_o}\right)^{1/n_1}. \quad \ldots\ldots\ldots\ldots\ldots (A\text{-}33)$$

σ is interfacial tension, σ_o is "initial" tension corresponding to the read-in capillary pressure curve, and n_1 is a read-in exponent generally in the range of 4 to 10. n_g, n_{og}, k_{rgcw}, k_{rocw}, S_{wir}, S_{org}, and S_{gr} are input data. As interfacial tension decreases, S_{gr}^* and S_{org}^* approach zero as

$$S_{gr}^* = f(\sigma)S_{gr} \quad \ldots\ldots\ldots\ldots\ldots (A\text{-}34)$$

and

$$S_{org}^* = f(\sigma)S_{org}. \quad \ldots\ldots\ldots\ldots\ldots (A\text{-}35)$$

Gas-phase relative permeability is treated with hysteresis as described elsewhere.[23] Thus, S_{gr}^* is also a function of $S_{g\max}$ and S_g when S_g is less than $S_{g\max}$, where $S_{g\max}$ is historical maximum gas saturation in the grid block.

For large n_1, as σ decreases below σ_o, the value of $f(\sigma)$ will remain near 1.0 until σ/σ_o is very small.

This means that k_{rg} and k_{rog}, given by Eqs. A-29 and A-30, will vary little with interfacial tension until close proximity to the critical point is attained. This reflects our understanding of the literature on low tension behavior, which indicates that very low interfacial tensions are necessary to reduce residual oil saturations appreciably under normal reservoir pressure gradients.

In summary, Eqs. A-29 through A-35 give k_{rg} and k_{rog} of specified curvature with specified residual saturations, S_{gr} and S_{org}, at original gas/oil interfacial tension. As tension decreases toward zero, the curves continuously approach straight lines with zero residual saturations.

If water is immobile, then $k_{rw}=0$ and $k_{ro}=k_{rocw}\times k_{rog}$, as described above. For the three-phase case,

$$k_{ro}=k_{rocw}\left[(k_{row}+k_{rw})(k_{rog}+k_{rg})-k_{rw}-k_{ro}\right], \quad \ldots\ldots\ldots\ldots\ldots\ldots \text{(A-36)}$$

which is Stone's method[24] modified slightly for the case where k_{rocw} is less than 1. Analytical relationships used for k_{rw} and k_{row} are

$$k_{rw}=k_{rwro}\left(\frac{S_w-S_{wir}}{1-S_{wir}-S_{orw}}\right)^{n_w} \quad \ldots\ldots\ldots \text{(A-37)}$$

and

$$k_{row}=\left(\frac{1-S_w-S_{orw}}{1-S_{wir}-S_{orw}}\right)^{n_{ow}} \quad \ldots\ldots\ldots\ldots \text{(A-38)}$$

Interfacial Tension and Capillary Pressure

The gas/oil interfacial tension is calculated from the Macleod-Sugden correlation,[16]

$$\sigma^{1/4}=\sum_{i=1}^{N_c} P_{chi}(\rho_L x_i-\rho_g y_i), \quad \ldots\ldots\ldots \text{(A-39)}$$

where P_{chi} is the parachor of Component i and densities (here only) are in units of gram-moles per cubic centimeter. If a gas cap is initially present in the reservoir, the σ_o is calculated from Eq. A-39 using the equilibrium phase densities and compositions. If the original reservoir oil is undersaturated, saturation (bubble-point) pressure is calculated and σ_o is calculated from Eq. A-39 using equilibrium phase densities and compositions at that pressure.

The read-in gas/oil capillary pressure curve is assumed to correspond to a tension of σ_o. At any other interfacial tension, the read-in P_{cgo} is multiplied by σ/σ_o. Input capillary pressures can be expressed in tabular or analytical form. In this work, we used analytical expressions

$$P_{cwo}=a_w+b_w(1-S_w)+c_w(1-S_w)^3 \quad \ldots \text{(A-40)}$$

and

$$p_{cgo}=a_g+b_gS_g+c_gS_g{}^3. \quad \ldots\ldots\ldots\ldots \text{(A-41)}$$

Viscosity Treatment

Water viscosity is a constant read as input data. Gas- and oil-phase viscosities are computed using the Lohrenz *et al.* method.[15] The phase densities in their method are obtained from the equation of state, so that gas- and oil-phase viscosities converge to a common value as phase compositions converge near a critical point.

Calculation of Critical Composition

The model formulation described in the body of this paper has been programmed in single-cell or zero-dimensional material balance mode. Two recent papers[25,26] discuss a rigorous method of critical pressure, temperature, and composition calculations. We have found that our problem is generally determination of critical composition at given pressure and temperature. We use this single-cell calculation for this purpose. A critical point is determined for a specified initial oil composition, specified pressure and temperature, and an injection gas composition having one degree of freedom. A series of gas injection runs is performed with the compositional "degree of freedom" varied. Each run simulates continued mixing of injected gas with the mixture resulting from gas and oil removal at constant pressure using relative permeability curves. By these trial-and-error runs, an injection composition is found that results in the cell's gas and oil phases converging at the critical composition. If injection gas is too lean, oil will disappear in the cell; if too rich, gas will disappear – in either case with a significant disparity between final equilibrium gas- and oil-phase compositions. This single-cell type of calculation is discussed in detail in the literature.[8-10] We simply point out here that we have found it provides a rather quick and reliable procedure for calculating a critical composition. In addition, of course, the calculation gives a close estimate (in our experience) of the "minimum enrichment" injection composition necessary to achieve MCM. Fussell *et al.*[9] discuss this in greater detail and point out that the shape of relative permeability curves used in this calculation can affect the accuracy of this indicated minimum enrichment.

SI Metric Conversion Factors

bbl	× 1.589 873	E−01	=	m^3
cp	× 1.0*	E−03	=	Pa·s
cu ft	× 2.831 685	E−02	=	m^3
°F	(°F−32)/1.8		=	°C
ft	× 3.048*	E−01	=	m
psi, psia	× 6.894 757	E+00	=	kPa
psi^{-1}	× 1.450 377	E−01	=	kPa^{-1}

*Conversion factor is exact.

SPEJ

Original manuscript received in Society of Petroleum Engineers office Sept. 23, 1979. Paper accepted for publication May 22, 1980. Revised manuscript received Aug. 6, 1980. Paper (SPE 8284) first presented at the SPE 54th Annual Technical Conference and Exhibition, held in Las Vegas, Sept. 23-26, 1979.